Inorganica Chimica Acta 392 (2012) 345–353

Contents lists available at SciVerse ScienceDirect

Inorganica Chimica Acta

journal homepage: www.elsevier.com/locate/ica

6-Benzhydryl-4-methyl-2-(1*H*-benzoimidazol-2-yl)phenol ligands and their zinc complexes: Syntheses, characterization and photoluminescence behavior

Zihong Zhou [a,d], Wen Li [a], Xiang Hao [b], Carl Redshaw [c,*], Langqiu Chen [d], Wen-Hua Sun [b,*]

[a] Key Laboratory of Photochemical Conversion and Optoelectronic Materials, Technical Institute of Physics and Chemistry, The Chinese Academy of Sciences, Beijing 100190, China
[b] Key Laboratory of Engineering Plastics and Beijing National Laboratory for Molecular Science, Institute of Chemistry, Chinese Academy of Sciences, Beijing 100190, China
[c] School of Chemistry, University of East Anglia, Norwich NR4 7TJ, UK
[d] Key Laboratory of Environmentally Friendly Chemistry and Application of Ministry of Education, College of Chemistry, Xiangtan University, Xiangtan 411105, China

ARTICLE INFO

Article history:
Received 18 January 2012
Received in revised form 26 March 2012
Accepted 30 March 2012
Available online 6 April 2012

Keywords:
6-Benzhydryl-4-methyl-2-(1*H*-benzoimidazol-2-yl)phenol
Zinc complexes
Fluorescence
UV-absorption spectra
ESIPT

ABSTRACT

The series of 6-benzhydryl-4-methyl-2-(1*H*-benzoimidazol-2-yl)phenol derivatives (H**L**) and their zinc complexes (Zn$\mathbf{L}_2$) were synthesized and fully characterized. Single-crystal X-ray diffraction studies were conducted on representative complexes (**C1** and **C4**), which revealed a distorted tetrahedral geometry at zinc. By comparison with these organic compounds (H**L**), the fluorescent quantum yields of the corresponding zinc complexes were increased. The fluorescence intensities of zinc complexes were affected by the solvents used, and enhanced intensities in methanol were observed compared with those observed in other solvents such as dichloromethane and toluene. The fluorescence decay mainly followed a single exponential in toluene, whereas a double exponential decay was observed in the presence of two active species in methanol and dichloromethane.

1. Introduction

The photophysical properties of various benzimidazole derivatives have been intensively studied in recent years, and their potential application in molecular electronics and biological fluorescence probing has been recognized [1–6]. In addition, a number of imidazole derivatives have been considered as inhibitors of copper corrosion [7–9]. With the potential for use as fluorescence probes in mind, the influence of the surrounding environment (the solvent) on the fluorescent properties has been considered [10–12]. In general, both pH values and the various substituents present impacted on the fluorescent properties of benzimidazole derivatives [13–17]. In view of this, herein new benzimidazole ligands containing a phenoxy group in combination with a bulky benzhydryl moiety have been prepared, and their zinc complexes were synthesized and characterized. Furthermore, the photophysical properties of both the organic and zinc compounds were investigated, which revealed that the intensities and size of the observed shifts relied on the coordination environment and the solvent.

2. Results and discussion

2.1. Synthesis and characterization

A series of 6-benzhydryl-4-methyl-2-(1*H*-benzoimidazol-2-yl)phenol derivatives was synthesized by the condensation reaction of 6-benzhydryl-4-methylsalicylaldehyde with the corresponding 2-aminoaniline or *N*-alkyl-2-nitroaniline (Scheme 1), and these ligands were fully characterized by FT-IR and NMR spectroscopy as well as by elemental analysis. Further reaction with 0.5 equivalents of zinc acetate in tetrahydrofuran (THF) afforded the zinc complexes bis(6-benzhydryl-4-methyl-2-(1*H*-benzoimidazol-2-yl)phenolate) in good yields (**C1**–**C6**, Scheme 1). The zinc complexes were characterized by FT-IR spectroscopy, elemental analysis and by single-crystal X-ray diffraction for the representative complexes **C1** and **C4**.

2.2. X-ray crystallographic study

Single crystals of complexes **C1** and **C4** suitable for X-ray structural determinations were grown by the slow diffusion of *n*-heptane into THF solutions. Both molecular structures (Figs. 1 and 2) revealed a distorted tetrahedral geometry at zinc, comprising of two monoanionic bidentate ligands; selected bond lengths and angles are tabulated in Table 1.

* Corresponding authors. Tel.: +86 10 62557955; fax: +86 10 62618239.
E-mail addresses: Carl.Redshaw@uea.ac.uk (C. Redshaw), whsun@iccas.ac.cn (W.-H. Sun).

0020-1693/$ - see front matter © 2012 Elsevier B.V. All rights reserved.
http://dx.doi.org/10.1016/j.ica.2012.03.057

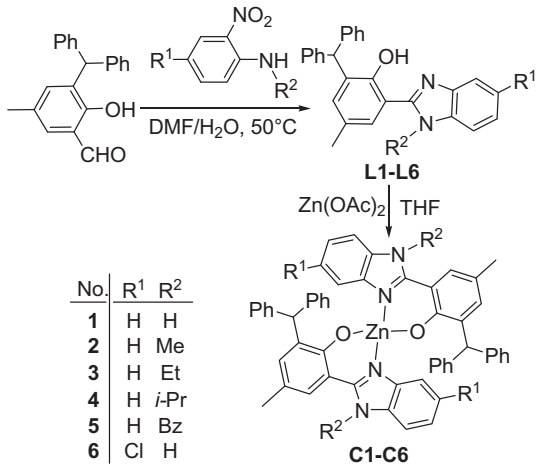

Scheme 1. Synthesis of organic compounds and their zinc complexes.

In the solid state of complex **C1**, there are two independent molecules, which interact via an intermolecular hydrogen bond between the benzimidazole N–H group and the phenol oxygen atom (N(4)···O(1a) = 2.842 Å). There are slight differences for the bond lengths and angles at zinc for the two ligands: for one ligand, Zn(1)–O(1) (1.918(3) Å), Zn(1)–N(1) (1.982(4) Å), and O(1)–Zn(1)–N(1) (94.52(15)°), whilst for the other ligand, Zn(1)–O(1a) (1.939(3) Å), Zn(1)–N(1a) (1.986(4) Å), and O(1a)–Zn(1)–N(1a) (94.41(16)°) (Table 1). In the molecular structure, the atoms O(1), Zn(1), and N(1) are almost coplanar with the phenolate and imidazolyl planes with individual dihedral angles of 166.6° and 169.3°, respectively, whereas the dihedral angles of the plane of atoms O(1a), Zn(1), and N(1a) with those of the other ligand are 149.5° and 162.3°, respectively. The planes formed by atoms O(1), Zn(1), and N(1) and O(1a), Zn(1), and N(1a) are almost vertical to each other with a dihedral angle of 88.1° (Fig. 1).

Similar to complex **C1**, the molecular structure of complex **C4** (Fig. 2) revealed a distorted tetrahedral geometry at zinc, however the two ligands exhibited equivalent bonding at zinc. The dihedral angles between the plane of atoms O(1), Zn(1), and N(1) with the planes of the imidazolyl and phenolate in complex **C4** are 150.3° and 156.6°, respectively, which are slightly smaller those observed in the complex **C1**. Similar coordination features around zinc were observed in the analogous complexes bearing

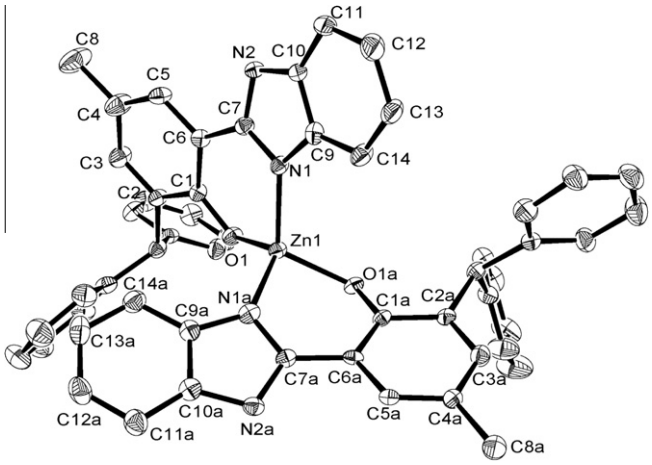

Fig. 1. ORTEP drawing of complex **C1** with thermal ellipsoids drawn at the 30% probability level. Hydrogen atoms are omitted for clarity (two independent molecules are included, only one structure is listed).

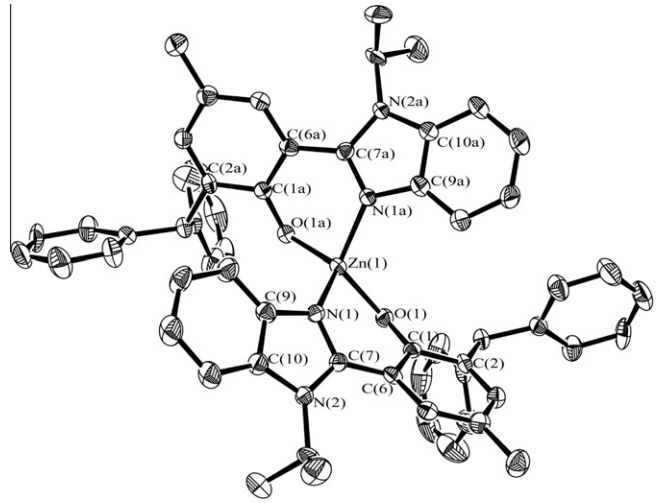

Fig. 2. ORTEP plot of **C4** with thermal ellipsoids drawn at the 30% probability level. Hydrogen atoms linked on carbon atoms have been omitted for clarity.

Table 1
Selected bond lengths (Å) and angles (°) for complexes **C1** and **C4**.

	C1	C4
Bond lengths (Å)		
Zn(1)–O(1)	1.918(3)	1.924(3)
Zn(1)–O(1a)	1.939(3)	1.924(3)
Zn(1)–N(1)	1.982(4)	1.990(4)
Zn(1)–N(1a)	1.986(4)	1.990(4)
N(1)–C(7)	1.319(6)	1.341(6)
N(1a)–C(7a)	1.327(6)	1.341(6)
N(1)–C(9)	1.383(6)	1.387(6)
N(1a)–C(9a)	1.386(6)	1.387(6)
O(1)–C(1)	1.326(6)	1.321(5)
O(1a)–C(1a)	1.329(5)	1.321(5)
N(2)–C(7)	1.358(6)	1.377(6)
N(2a)–C(7a)	1.355(6)	1.377(6)
C(6)–C(7)	1.476(7)	1.470(6)
C(6a)–C(7a)	1.466(7)	1.470(6)
Bond angles (°)		
O(1)–Zn(1)–O(1a)	117.32(14)	121.4(2)
O(1)–Zn(1)–N(1)	94.52(15)	93.32(14)
O(1a)–Zn(1)–N(1)	114.72(15)	119.36(15)
O(1)–Zn(1)–N(1a)	117.86(16)	119.36(15)
O(1a)–Zn(1)–N(1a)	94.41(16)	93.32(14)
N(1)–Zn(1)–N(1a)	119.87(17)	111.8(2)

2-(1*H*-benzoimidazol-2-yl)phenolate, which though they lacked the bulky 6-benzhydryl group [18], did possess π–π stacking interactions. The bulky substituents present for the ligands herein, prevented the formation of π–π stacking interactions for **C1** and **C4**.

2.3. Absorption spectra

The UV–Vis spectra of the 6-benzhydryl-4-methyl-2-(1*H*-benzoimidazol-2-yl)phenol ligands (H**L**, **L1**–**L6**) and their zinc complexes (Zn$\mathbf{L}_2$) were each measured in anhydrous methanol, dichloromethane and toluene solutions; the spectral characteristics are tabulated in Table 2. The absorptions of the compounds were significantly affected by the solvent employed. For example, all organic compounds (**L1**–**L6**) exhibited absorption peaks at around 225 nm in methanol, 230 nm in dichloromethane, and 330 nm in toluene solutions, indicating that their absorptions were blue-shifted on increasing the polarity of the solvent. These could be assigned to π–π* transitions on the basis of the extinction

Table 2
UV–Vis absorption properties of **L1**–**L6** and **C1**–**C6**.

Media	Ligands	$\lambda_{abs-max}$ (nm)	$\varepsilon_{(\lambda max)}$ (M^{-1} cm^{-1})	Complexes	$\lambda_{abs-max}$ (nm)	$\varepsilon_{(\lambda max)}$ (M^{-1} cm^{-1})
Methanol	**L1**	224	33980	**C1**	224	32454
CH_2Cl_2		231	22888		234	40380
Toluene		332	17400		301	25080
Solid		415	–		393	–
Methanol	**L2**	223	30646	**C2**	229	37048
CH_2Cl_2		231	26224		234	39946
Toluene		332	16106		299	34416
Solid		408	–		391	–
Methanol	**L3**	222	32396	**C3**	221	26590
CH_2Cl_2		231	21382		233	38494
Toluene		333	16782		298	18826
Solid		398	–		393	–
Methanol	**L4**	221	33408	**C4**	221	8186
CH_2Cl_2		232	29522		235	42080
Toluene		327	15488		297	29258
Solid		384	–		377	–
Methanol	**L5**	220	31714	**C5**	234	39480
CH_2Cl_2		233	33958		234	38574
Toluene		333	19292		300	22636
Solid		418	–		389	–
Methanol	**L6**	225	32010	**C6**	223	10258
CH_2Cl_2		231	24480		236	44282
Toluene		336	14526		306	21552
Solid		407	–		384	–

coefficients ($\varepsilon_{(\lambda max)}$, Table 2). The dipolar interactions and the protonation at the basic sp^2-N centers led to red-shifts; whereas the protonation of the hydroxyl group of the phenol derivatives resulted in blue-shifts. Such phenomena were consistent with observations reported in the literature [19–21].

By comparison to the organic compounds, the absorption bands of all the zinc complexes were strongly enhanced and shifted with the same trends according to the polarity of the solvent used. As shown in Fig. 3, the UV-absorption spectra (A) of all compounds in toluene were shifted to the red in comparison to those of the corresponding compounds in dichloromethane (B); the red-shifts were about 100 nm for the organic compounds (**L1**–**L6**), and 70 nm for the zinc complexes (**C1**–**C6**).

The solvent polarity affected the energy gap and the electronic transitions due to the excited-state species possessing a large dipole moment and facile electronic reorganization. The energy gap (ΔE) between the ground state and the excited state was gradually enlarged on increasing the polarity of the solvent used ($\Delta E_p > \Delta E_n$) (Scheme 2) [22,23]. In the solid thin films, all the zinc complexes (**C1**–**C6**) showed significantly blue-shifted absorptions compared to those of the corresponding ligands (**L1**–**L6**) [24–26].

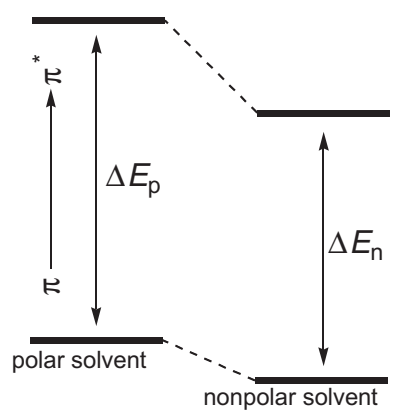

Scheme 2. The effect of solvent on the electronic transition energies.

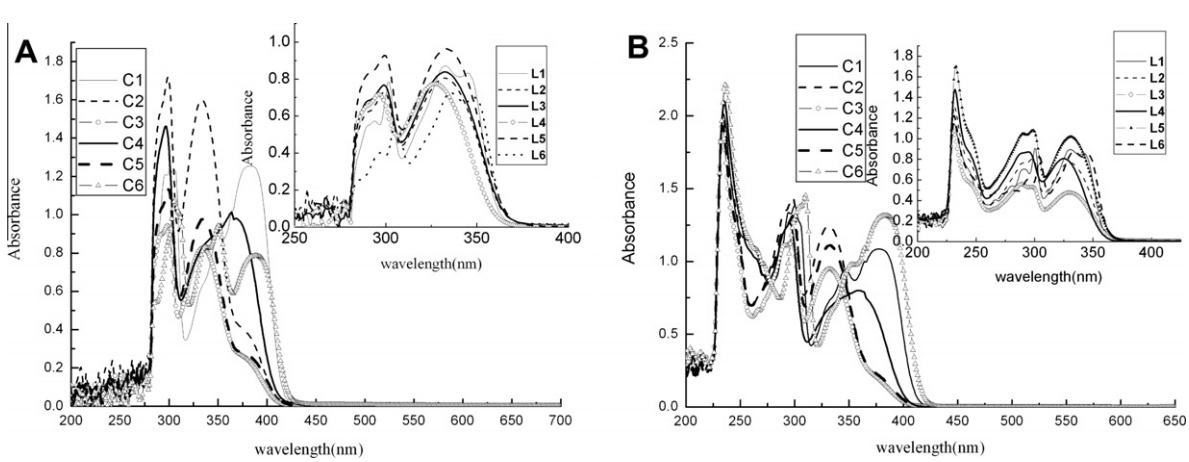

Fig. 3. UV-absorption spectra of complexes Zn**L**$_2$ and corresponding ligands H**L** in solution (5×10^{-5} M) of toluene (A) and dichloromethane (B).

2.4. Fluorescence spectra and quantum yields

Fluorescence spectra (Fig. 4) of all compounds were obtained in different solvents, which were selected for their different polarities and potential for hydrogen bonding, data are collected in Table 3. On comparing the absorptions for the ligands versus the corresponding zinc complexes, it was evident that coordination to zinc of the monoanionic ligand sets resulted in significant blue-shifts. The blue-shifted absorptions were the result of increased π-electron donation through the coordination of the Zn(II) to the anionic ligands, i.e. the electron was transferred to the vacant orbitals of Zn(II). In addition, on increasing the polarity of solvent used, the fluorescence emission and fluorescence excitation spectra of all the ligands (**L1**–**L6**) were in general blue-shifted. Interestingly, using dichloromethane or toluene as solvent (Fig. 4D and F), complexes **C1**, **C4**, and **C6** showed larger fluorescence quantum yield (Φ_F) than their analogs **C2**, **C3**, and **C5**.

In methanol, the intensities of the large Stokes-shifted fluorescence for the ligands were reduced because of the intermolecular hydrogen bonding interactions inhibiting the ESIPT process in H**L**; exceptions were **L1** and **L6** (Fig. 5, Stokes shifts 153 and 159 nm, respectively, Table 3). The influence of methanol on **L1** and **L6**, both of which possess an –NH group at the benzoimidazole, was different due to the differing protonation/hydroxyl interactions of the methanol with these ligands (Scheme 3).

The emissions of **L2**, **L3**, **L4** and **L5** for the Stokes shift showed bands at 146, 152, 157 and 150 nm belonging to ESIPT in MeOH. There were lower Stokes shift bands alongside the ESIPT bands,

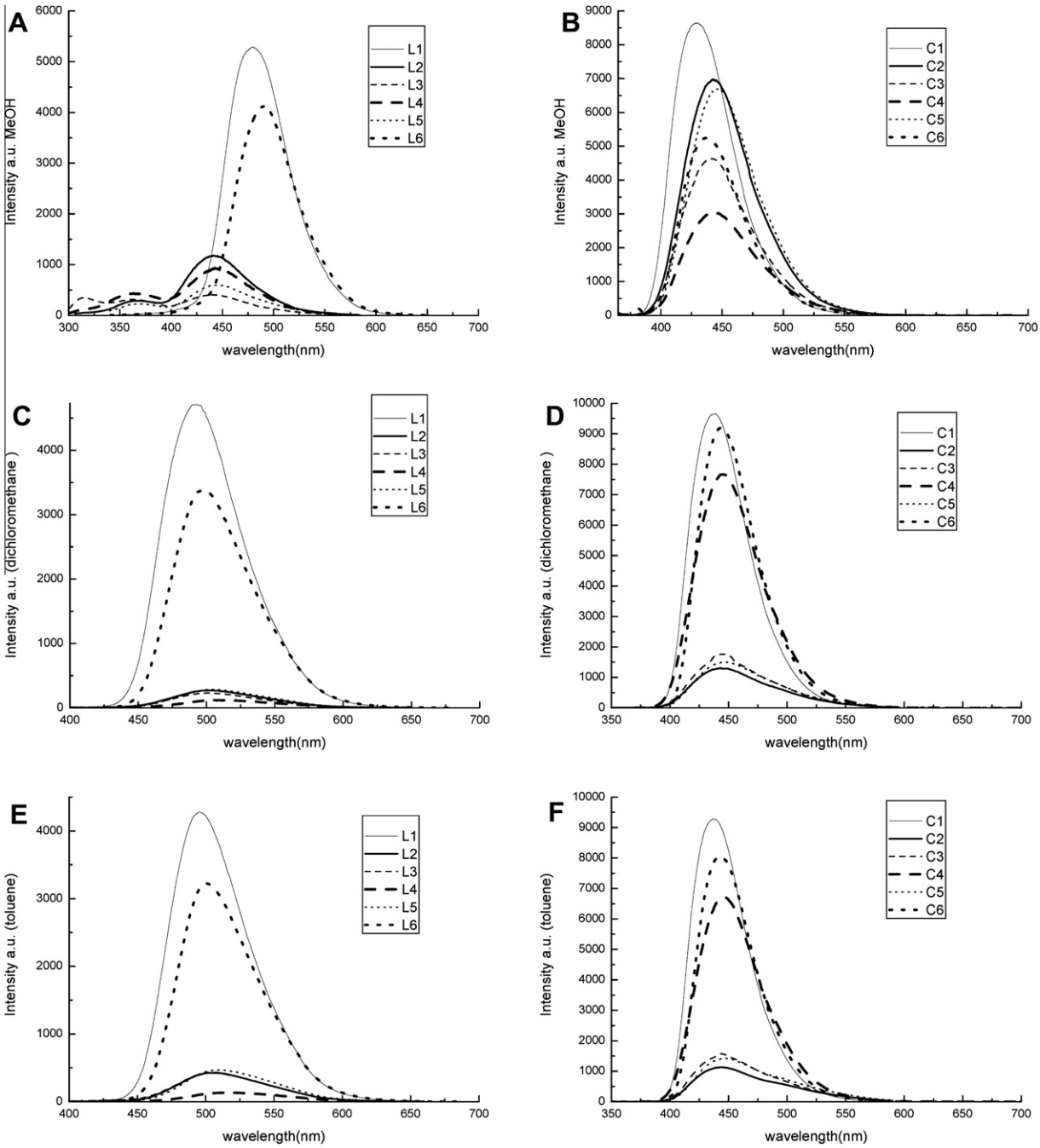

Fig. 4. Fluorescence spectra of ligands H**L** and zinc complexes Zn**L**$_2$ in solution (5×10^{-5} M) of anhydrous methanol (A and B), dichloromethane (C and D) and toluene (E and F).

Table 3
Emission data for compounds **L1**–**L6** and **C1**–**C6**.

Media		Ligands				Complexes		
		λ_{maxEm} (nm)	λ_{Ex} (nm)	$\Delta\lambda^a$ (nm)		λ_{maxEm} (nm)	λ_{Ex} (nm)	$\Delta\lambda^a$ (nm)
Methanol	**L1**	481	328	153	**C1**	431	365	66
CH_2Cl_2		489	330	159		439	380	59
Toluene		496	345	151		437	380	57
Solid		498	415	83		462	393	69
Methanol	**L2**	**442**, **365**	**296**	**146**, **69**	**C2**	443	353	90
CH_2Cl_2		500	330	170		442	300	142
Toluene		504	335	169		444	300	144
Solid		487	408	79		467	391	76
Methanol	**L3**	**441**, **361**	**289**	**152**, **72**	**C3**	440	355	85
CH_2Cl_2		503	330	173		444	300	144
Toluene		507	335	172		444	300	144
Solid		493	398	95		431	393	38
Methanol	**L4**	**443**, **363**	**286**	**157**, **77**	**C4**	442	350	92
CH_2Cl_2		509	330	179		445	360	85
Toluene		518	330	188		445	370	75
Solid		496	384	112		437	397	40
Methanol	**L5**	**447**, **370**	**297**	**150**, **73**	**C5**	446	355	91
CH_2Cl_2		506	330	176		445	300	145
Toluene		510	335	175		448	300	148
Solid		492	418	74		435	389	46
Methanol	**L6**	490	331	159	**C6**	437	372	65
CH_2Cl_2		497	345	152		444	380	64
Toluene		501	350	151		443	390	53
Solid		499	407	92		430	384	46

[a] $\Delta\lambda$ = stokes shift.

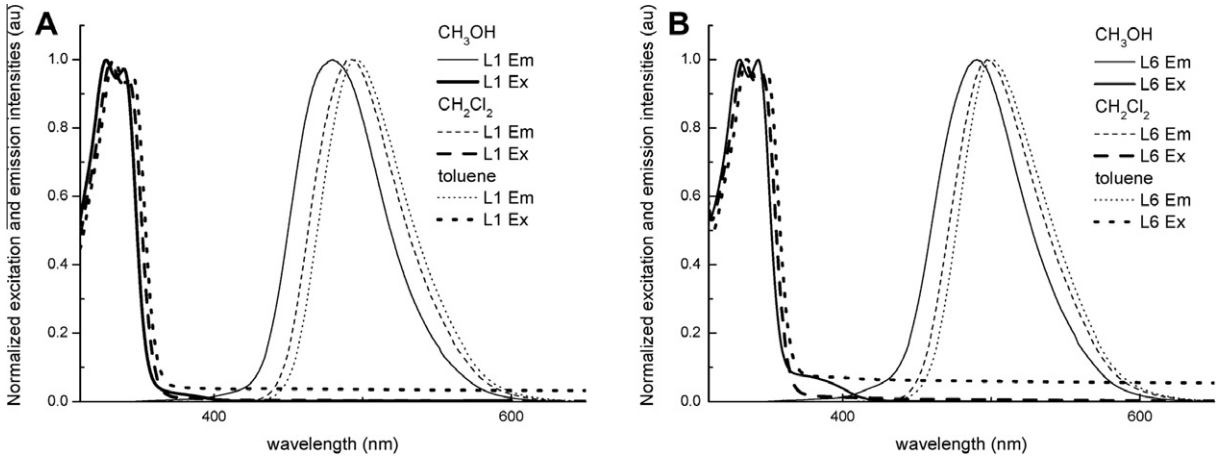

Fig. 5. Normalized excitation and emission spectra of **L1** (A) and **L6** (B) in different solvents.

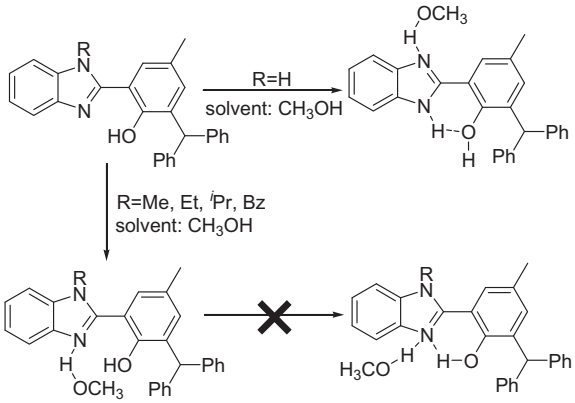

Scheme 3. The proposed protonation of methanol with the ligands.

which corresponded to significant primary photo-relaxation for **L2**, **L3**, **L4** and **L5** in methanol (Table 3). Such unusual phenomena were caused by the synergic influence of the excited enol-configuration and the excited keto-configuration [27,28]. For all ligands (**L1**–**L6**), the rapid excited-state intramolecular proton-transfer (ESIPT) occurred through the *cis*-enol structure, with intramolecular hydrogen-bonding between the phenol and the $N_{imidazole}$ atom (Scheme 4). Compared with the ligands, less blue-shifts were observed within the spectra of the corresponding zinc complexes, consistent with literature observations [29–31]. In all cases, the photo-excitation of the closed *cis*-enol form resulted in ESIPT to form the excited state keto form, illustrating the large Stokes shifted emission [29,32,18,33]. The emission spectra of all ligands in the solid state were measured at room temperature (Table 3), and showed photoluminescence peaks at about 500 nm; which were generally similar to the values observed in solution.

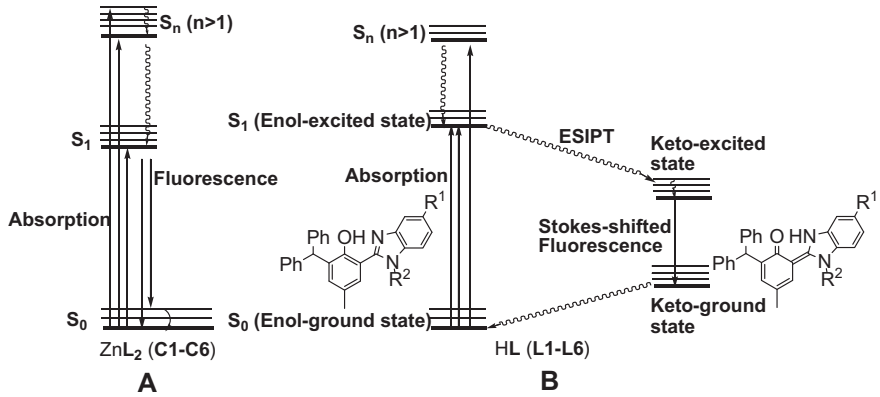

Scheme 4. Electronic transitions in the photo-luminescent process for the zinc complexes (A) and ligands (B).

Table 4
Excited singlet state lifetimes (ns) and the values of radiative decay rate (k_r) of ligands (**L1**–**L6**) and zinc complexes (**C1**–**C6**).

Media		Ligands						Complexes				
		Φ_F	τ_1 (ns)	k_{r1}[a] (S^{-1})	τ_2 (ns)	k_{r2}[a] (S^{-1})		Φ_F	τ_1 (ns)	k_{r1}[a] (S^{-1})	τ_2 (ns)	k_{r2}[a] (S^{-1})
Methanol	**L1**	0.06	3.2	1.88	–	–	**C1**	0.10	3.2	3.13	–	–
CH_2Cl_2		0.07	3.8	1.84	–	–		0.09	3.3	2.73	–	–
Toluene		0.07	4.1	1.71	–	–		0.09	3.4	2.65	–	–
Methanol	**L2**	0.016	4.8(37.7)	0.33	2.8(62.3)	0.57	**C2**	0.13	3.8	3.42	–	–
CH_2Cl_2		0.005	4.3(5.2)	0.12	0.6(94.8)	0.83		0.01	1.6(17.6)	0.63	4.4(82.4)	0.23
Toluene		0.01	0.8	1.25	–	–		0.01	4.1(71.5)	0.24	1.6(28.5)	0.63
Methanol	**L3**	0.007	3.8(83.5)	0.18	1.1(16.5)	0.64	**C3**	0.16	4.5(34.8)	3.56	2.8(65.2)	5.71
CH_2Cl_2		0.005	0.6(83.5)	0.83	2.7(16.5)	0.19		0.02	4.3(74.0)	0.47	1.2(26.0)	1.67
Toluene		0.01	0.8	1.25	–	–		0.02	3.9(76.3)	0.51	1.3(23.7)	1.54
Methanol	**L4**	0.008	1.9(23.1)	0.42	4.0(76.9)	0.20	**C4**	0.17	4.1(83.5)	4.15	2.0(16.5)	8.50
CH_2Cl_2		0.002	3.2	0.06	–	–		0.12	4.2(82.8)	2.86	1.6(17.2)	7.60
Toluene		0.003	2.6(10.2)	0.12	0.5(89.8)	0.60		0.16	3.7	4.32	–	–
Methanol	**L5**	0.009	3.7	0.24	–	–	**C5**	0.13	4.0	3.25	–	–
CH_2Cl_2		0.004	0.6	0.67	–	–		0.02	1.6(21.2)	1.25	4.6(78.8)	0.43
Toluene		0.01	0.9	1.11	–	–		0.02	1.2(20.7)	1.67	4.0(79.3)	0.50
Methanol	**L6**	0.06	3.6	1.67	–	–	**C6**	0.19	1.9(11.4)	10.0	3.8(88.6)	6.00
CH_2Cl_2		0.05	7.1(8.4)	0.70	3.0(91.6)	1.67		0.08	2.0(14.0)	4.00	3.9(86.0)	2.05
Toluene		0.08	3.7	2.16	–	–		0.08	3.5	2.29	–	–

Concentration: 5×10^{-5} M.
[a] $k_r = \Phi_F/\tau$ ($S^{-1} = 10^7\ s^{-1}$).

According to Table 3, all ligands (**L1**–**L6**) showed small Stokes shift in the solid state in comparison to their respective solutions, indicating that the ESIPT does not occur in the solid state.

The fluorescence decay was observed by using excitation at 330 or 350 nm (laser), and the results are listed in Table 4. The fluorescence decay followed a single exponential in toluene for all compounds, with the exception of compounds **L4**, **C2**, **C3**, and **C5**. Using methanol or dichloromethane as solvent, double exponential decay was mostly observed. The two different lifetimes were caused by the presence of different excited state species due to the conversion rate of the two species being slower than the emission rate, indicating that these species were not in equilibrium [34]. In another word, there was one kind of species present in toluene, but two kinds of species present in the other solvents used herein [21,35].

The fluorescence intensities of the zinc complexes Zn**L**$_2$ were significantly enhanced on comparison to those of the corresponding ligands (H**L**). Compared to **L2**–**L5**, compounds **L1** and **L6** having a N–H group, exhibited stronger fluorescent intensity due to intramolecular hydrogen bonding. In methanol solution, the quantum yields of the zinc complexes were increased because the bulky substituents present slowed down the rate of radiationless decay, consistent with previous observations [36,37]. Meanwhile, the intermolecular hydrogen bonds (with methanol) resulted in increased planarity of the atoms C(6), C(7), O(1), Zn(1), N(I), and C(1).

3. Conclusion

The series of 6-benzhydryl-4-methyl-2-(1*H*-benzoimidazol-2-yl)phenol derivatives (H**L**) and their zinc complexes (Zn**L**$_2$) were synthesized and fully characterized. The molecular structures of the complexes **C1** and **C4** exhibited distorted tetrahedral geometry at zinc. The maximum UV-absorption bands of both the organic (H**L**) were blue-shifted on increasing the polarity of the solvent used. By comparison with the organic compounds (H**L**), the fluorescent quantum yields of the corresponding zinc complexes were increased. The fluorescence intensities of the zinc complexes were heavily affected by the solvents used, with better intensities observed in methanol than in other solvents such as dichloromethane and toluene. The fluorescence decay mainly followed a single exponential in toluene, whereas in methanol and dichloromethane, the double exponential decay was observed indication the presence of two active species.

4. Experimental

4.1. General consideration

All manipulations of air and/or moisture-sensitive compounds were carried out under an atmosphere of nitrogen using standard Schlenk techniques. THF was refluxed over sodium-benzophenone and distilled under nitrogen prior to use. 3-Benzhydryl-2-hydroxy-5-methylbenzaldehyde was prepared according to the literature method [38]. All aniline derivatives were purchased and used as the obtained. ^{1}H and ^{13}C NMR spectra were recorded on a Bruker DMX400 MHz instrument at ambient temperature using TMS as an internal standard. Absorption spectra were determined on a SHIMADZU UV-1601PC UV–Vis Spectrophotometer. IR spectra were recorded on a Perkin–Elmer System 2000 FT-IR spectrometer using a KBr disc in the range of 400–4000 cm^{-1}. Elemental analyses were performed on a Flash EA 1112 microanalyzer. The steady-state fluorescent spectra were measured on an F4500-FL fluorescence spectrophotometer; fluorescence lifetimes were obtained using the time-correlated single-photon counting technique (Edinburgh Analytical Instruments F900 fluorescence spectrofluorimeter). Thin films of the samples were prepared on quartz slides (1 cm) through spin-coating. Fluorescence quantum yields (Φ_F) were calculated according to the comparative method, using anthracene in methanol (Φ_F = 0.29) as a standard [27,39–41].

$$\Phi_{F,x} = \Phi_{F,s}\frac{\int I_{F,x}(v)dv \cdot (1-10^{-As}) \cdot (n_x)^2}{\int I_{F,s}(v)dv \cdot (1-10^{-Ax}) \cdot (n_s)^2}$$

where $\Phi_{F,s}$ is the quantum yield of standard, integrals $\int I_{F,x}(v)dv$ and $\int I_{F,s}(v)dv$ are the areas under curves of the sample and standard, $I_{F,x}(v)$ and $I_{F,s}(v)$ are fluorescence intensities at wavelength for the sample and the standard, respectively. A_x and A_s are absorptions of the sample and standard, n_x and n_s are refractive indices of the solvents.

4.2. Preparation of ligands

4.2.1. 6-Benzhydryl-4-methyl-2-(benzoimidazol-2-yl)phenol (*L1*)

A modified synthetic procedure for the *ortho*-nitroaniline derivatives (1.21 g, 11.2 mmol) was employed: DMF/H_2O = 4:1 (80 mL:20 mL), sodium hydrosulfite (10.1 g, 58.3 mmol), 3-benzhydryl-2-hyd roxy-5-methylbenzaldehyde (3.38 g, 11.2 mmol) were combined under nitrogen. The reaction mixture was refluxed for 5 h. The solvent was then removed *in vacuo*, and the resultant residue was dissolved with dichloromethane. The combined organic extracts were dried and purified on an alumina column using petroleum ether/ethyl acetate (v/v = 25:1) as the eluent to obtain the target compound as a white powder in 16.7% (0.76 g, 1.87 mmol) yield. mp 241−242 °C, IR (KBr; cm^{-1}): ν 3382, 3025, 2921, 1628, 1596, 1525, 1448, 1383, 1252, 1073, 739, 690. ^{1}H NMR ($CDCl_3$, 400 MHz, TMS): δ 7.53 (m, 2H), 7.31–7.16 (m, 13H), 6.77 (s, 1H), 6.08 (s, 1H), 2.24 (s, 3H). ^{13}C NMR ($CDCl_3$, 100 MHz, TMS): δ 14.34, 20.94, 49.89, 60.65, 111.45, 123.35, 123.44, 126.37, 128.42, 129.62, 132.94, 133.67, 143.59, 151.61, 154.60. *Anal.* Calc. for $C_{27}H_{22}N_2O$: C, 83.05; H, 5.68; N, 7.17. Found: C, 82.97; H, 5.72; N, 7.02%.

4.2.2. 2-Benzhydryl-4-methyl-6-(1-methyl-benzoimidazol-2-yl)phenol (*L2*)

Using the same procedure as for the synthesis of **L1**, but using a solution of *N*-methyl-2-nitrobenzenamine (1.46 g, 9.63 mmol) and 3-benzhydryl-2-hydroxy-5-methylbenzaldehyde (2.91 g, 9.63 mmol) in DMF/H_2O = 4:1 (80 mL:20 mL) was treated with about 5.2 equivalents of sodium hydrosulfite (8.73 g, 50.2 mmol) under nitrogen. **L2** was obtained as a yellow powder in 22.1% (0.86 g, 2.13 mmol) yield. mp 200–201 °C, IR (KBr; cm^{-1}): ν 3362, 3019, 1601, 1583, 1519, 1469, 1397, 1375, 1247, 1078, 741, 621. ^{1}H NMR ($CDCl_3$, 400 MHz, TMS): δ 7.67 (d, J = 7.46 Hz, 1H), 7.38−7.17 (m, 14H), 6.79 (s, 1H), 6.09 (s, 1H), 4.02 (s, 3H), 2.28 (s, 3H). ^{13}C NMR ($CDCl_3$, 100 MHz, TMS): δ 21.27, 33.27, 50.10, 109.60, 112.63, 118.84, 123.06, 123.28, 125.84, 126.27, 126.91, 128.37, 129.62, 132.86, 133.12, 135.86, 140.52, 143.77, 152.19, 154.62. *Anal.* Calc. for $C_{28}H_{24}N_2O$: C, 83.14; H, 5.98; N, 6.93. Found: C, 83.05; H, 6.04; N, 6.79%.

4.2.3. 2-Benzhydryl-6-(1-ethyl-benzoimidazol-2-yl)-4-methylphenol (*L3*)

Using the above procedure as for the synthesis of **L2**, but using *N*-ethyl-2-nitrobenzenamine (1.31 g, 7.92 mmol), 3-benzhydryl-2-hydroxy-5-methylbenzaldehyde (2.39 g, 7.92 mmol), and sodium hydrosulfite (7.18 g, 41.2 mmol) was added, respectively. **L3** was as a yellow powder in 30.2% (0.85 g, 2.03 mmol) yield. mp 155–156 °C, IR (KBr; cm^{-1}): ν 3375, 3022, 1599, 1579, 1493, 1468, 1398, 1378, 1246, 1076, 741, 696. ^{1}H NMR ($CDCl_3$, 400 MHz, TMS): δ 7.66 (d, J = 7.38 Hz, 1H), 7.42 (d, J = 7.50 Hz, 1H), 7.32–7.09 (m, 11H), 6.80 (s, 1H), 6.50 (s, 1H), 6.09 (s, 1H), 5.67 (s, 1H), 4.48-4.43 (q, 2H), 2.28 (s, 3H), 1.64 (t, J = 7.2 Hz, 3H). ^{13}C NMR ($CDCl_3$, 100 MHz, TMS): δ 15.34, 21.14, 21.35, 40.72, 50.15, 51.24, 109.74, 112.64, 118.95, 123.06, 123.27, 125.20, 126.26, 126.99, 128.37, 128.63, 129.48, 129.51, 129.63, 130.97, 132.99, 133.12, 135.00, 140.69, 142.89, 143.81, 151.60, 154.65. *Anal.* Calc. for $C_{29}H_{26}N_2O$: C, 83.22; H, 6.26; N, 6.69. Found: C, 83.15; H, 6.33; N, 6.35%.

4.2.4. 2-Benzhydryl-6-(1-isopropyl-benzoimidazol-2-yl)-4-methylphenol (*L4*)

Using the above procedure, but using *N*-isopropyl-2-nitrobenzenamine (2.33 g, 12.9 mmol) was used instead of *N*-ethyl-2-nitrobenzenamine, reaction with 3-benzhydryl-2-hydroxy-5-methylbenzaldehyde (3.90 g, 12.9 mmol) and sodium hydrosulfite (11.7 g, 67.2 mmol). The product was obtained as a yellow powder in 13.6% (0.76 g, 1.76 mmol) yield. mp 158–159 °C, IR (KBr; cm^{-1}): ν 3341, 3054, 2910, 1599, 1493, 1441, 1391, 1367, 1244, 1069, 740, 699. ^{1}H NMR ($CDCl_3$, 400 MHz, TMS): δ 7.72 (d, J = 7.50 Hz, 1H), 7.66 (d, J = 7.52 Hz, 1H), 7.34–7.13 (m, 11H), 6.83 (s, 1H), 6.53 (s, 1H), 6.12 (s, 1H), 5.70 (s, 1H), 5.22 (m, 1H), 2.30 (s, 3H), 1.75 (d, J = 6.88 Hz, 6H). ^{13}C NMR ($CDCl_3$, 100 MHz, TMS): δ 21.14, 21.28, 21.60, 50.10, 51.24, 112.86, 113.32, 119.52, 122.65, 126.22, 126.29, 126.72, 127.24, 128.37, 128.62, 129.51, 129.64, 130.97, 133.01, 133.15, 142.13, 142.89, 143.72, 151.78, 153.86. *Anal.* Calc. for $C_{30}H_{28}N_2O$: C, 83.30; H, 6.52; N, 6.48. Found: C, 83.24; H, 6.67; N, 6.30%.

4.2.5. 2-Benzhydryl-6-(1-benzyl-benzoimidazol-2-yl)-4-methylphenol (*L5*)

Following the same procedure described for the formation of **L4**, treatment of *N*-benzyl-2-nitrobenzenamine (1.70 g, 7.47 mmol), 3-benzhydryl-2-hydroxy-5-methylbenzaldehyde (2.26 g, 7.47 mmol), and sodium hydrosulfite (6.78 g, 39.0 mmol) gave **L5** (0.52 g, 2.28 mmol, 14.5%). mp 196–197 °C, IR (KBr; cm^{-1}): ν 3026, 2913, 1605, 1496, 1444, 1397, 1250, 1155, 740, 691. ^{1}H NMR ($CDCl_3$, 400 MHz, TMS): δ 7.71 (d, J = 7.71 Hz, 1H), 7.38–7.14 (m, 18H), 7.10 (s, 1H), 6.74 (s, 1H), 6.08 (s, 1H), 5.60 (s, 2H), 2.04 (s, 3H). ^{13}C NMR ($CDCl_3$, 100 MHz, TMS): δ 20.97, 35.16, 50.10, 110.16, 112.19, 119.04, 123.39, 123.66, 125.73, 125.99, 126.27, 127.08, 128.10, 128.36, '129.40, 132.84, 133.27, 135.94, 136.39, 140.82, 143.76, 152.64, 154.53. *Anal.* Calc. for $C_{34}H_{28}N_2O$: C, 84.97; H, 5.87; N, 5.83. Found: C, 84.68; H, 5.94; N, 5.79%.

*4.2.6. 2-Benzhydryl-6-(5-chloro-benzoimidazol-2-yl)-4-methylphenol (**L6**)*

Using the same procedure as for the synthesis of **L1**, the reaction of 5-chloro-2-nitrobenzenamine (2.02 g, 11.7 mmol), 3-benzhydryl-2-hydroxy-5-methylbenzaldehyde (3.53 g, 11.7 mmol) and sodium hydrosulfite (10.6 mmol, 60.9 mol) gave **L6** (0.67 g, 3.90 mmol, 13.5%). mp 232–233 °C, IR (KBr; cm^{-1}): ν 3384, 3027, 2920, 1582, 1519, 1494, 1441, 1374, 1247, 1102, 1059, 738, 701. ^1H NMR ($CDCl_3$, 400 MHz, TMS): δ 8.05 (s, 1H), 7.31–7.17 (m, 13H), 6.78 (s, 1H), 6.07 (s, 1H), 2.24 (s, 3H). ^{13}C NMR ($CDCl_3$, 100 MHz, TMS): δ 20.97, 50.10, 110.16, 112.19, 119.04, 123.39, 123.66, 125.73, 125.99, 126.27, 127.08, 128.10, 128.36, 129.40, 129.61, 132.84, 133.27, 135.94, 136.39, 140.82, 143.76, 152.64, 154.53. *Anal.* Calc. for $C_{27}H_{21}ClN_2O$: C, 76.32; H, 4.98; N, 6.59. Found: C, 76.19; H, 5.11; N, 6.39%.

4.3. Preparation of zinc complexes

*4.3.1. Zinc di(6-benzhydryl-4-methyl-2-(benzoimidazol-2-yl)phenolate) (**C1**)*

To a stirred solution of **L1** (0.19 g, 0.5 mmol) in THF (15 mL) at room temperature, zinc acetate dihydrate 0.056 g (0.25 mmol) was added. The reaction mixture was stirred at room temperature for 12 h, and petroleum ether was added to precipitate the complex. The resulting precipitate was filtered, washed with petroleum ether, and dried under vacuum to furnish the product **C1** as a white powder in 81% (0.17 g, 0.21 mmol) yield. IR (KBr; cm^{-1}): ν 3612, 3057, 2967, 1625, 1599, 1531, 1451, 1335, 1248, 1081, 739, 670. *Anal.* Calc. for $C_{54}H_{42}N_4O_2Zn$: C, 76.82; H, 5.01; N, 6.64. Found: C, 76.73; H, 4.89; N, 6.57%.

*4.3.2. Zinc di(6-benzhydryl-4-methyl-2-(1-methyl-benzoimidazol-2-yl)phenolate) (**C2**)*

Using the same procedure as for the synthesis of **C1**, but using **L2** (0.20 g, 0.5 mmol), to which zinc acetate dihydrate 0.056 g (0.25 mmol) was added at room temperature, thereby affording **C2** in 95% (0.21 g, 0.25 mmol) yield. IR (KBr; cm^{-1}): ν 3727, 3023, 1553, 1470, 1444, 1398, 1325, 1247, 1077, 741, 696. *Anal.* Calc. for $C_{56}H_{46}N_4O_2Zn$: C, 77.10; H, 5.31; N, 6.42. Found: C, 77.01; H, 5.36; N, 6.39%.

*4.3.3. Zinc di(6-benzhydryl-4-methyl-2-(1-ethyl-benzoimidazol-2-yl)phenolate) (**C3**)*

As above, but using a solution of ligand **L3** (0.21 g, 0.5 mmol) in THF (15 mL), which was added zinc acetate dihydrate 0.056 g (0.25 mmol) at room temperature, to afford **C3** in 72.7% (0.16 g, 0.18 mmol) yield. IR (KBr; cm^{-1}): ν 3550, 3026, 1590, 1552, 1443, 1399, 1334, 1239, 1076, 747, 695. *Anal.* Calc. for $C_{58}H_{50}N_4O_2Zn$: C, 77.37; H, 5.60; N, 6.22. Found: C, 77.40; H, 5.44; N, 6.17%.

*4.3.4. Zinc di(6-benzhydryl-4-methyl-2-(1-isopropyl-benzoimidazol-2-yl)phenolate) (**C4**)*

The procedures are similar to that for **C3**, but using **L4** (0.22 g, 0.5 mmol), resulting in **C4** in 78.3% (0.18 g, 0.20 mmol) yield. IR (KBr; cm^{-1}): ν 3785, 3026, 2975, 1604, 1549, 1491, 1437, 1413, 1373, 1246, 1073, 748, 696. *Anal.* Calc. for $C_{60}H_{54}N_4O_2Zn$: C, 77.61; H, 5.86; N, 6.03. Found: C, 77.35; H, 5.79; N, 5.97%.

*4.3.5. Zinc di(6-benzhydryl-4-methyl-2-(1-benzyl-benzoimidazol-2-yl)phenolate) (**C5**)*

The procedure was similar to that for **C4**, but using **L5** (0.23 g, 0.48 mmol), leading to **C5** in 83.3% (0.20 g, 0.20 mmol) yield. IR (KBr; cm^{-1}): ν 3938, 3027, 2918, 1553, 1496, 1443, 1398, 1252, 1155, 733, 697. *Anal.* Calc. for $C_{68}H_{54}N_4O_2Zn$: C, 79.71; H, 5.31; N, 5.47. Found: C, 79.69; H, 5.11; N, 5.37%.

Table 5
Summary of crystallographic data for **C1** and **C4**.

	C1	**C4**
Empirical formula	$C_{54}H_{42}N_4O_2Zn$	$C_{60}H_{54}N_4O_2Zn$
Formula weight	844.29	928.46
Crystal system	monoclinic	monoclinic
Space group	$P2(1)/c$	$C2/C$
a (Å)	13.942(3)	16.626(3)
b (Å)	21.575(4)	10.260(2)
c (Å)	36.686(7)	28.932(6)
α (°)	90.00	90.00
β (°)	94.56(3)	99.36(3)
γ (°)	90.00	90.00
V (Å^3)	11000(4)	4869.6(16)
Z	8	4
D_{calcd} (g cm^{-3})	1.020	1.266
μ (mm^{-1})	0.484	0.553
T (K)	173(2)	293(2)
$F(000)$	3520	1952
θ Range (°)	1.10–25.34	1.43–27.47
Number of reflections collected	70616	18011
Number of unique reflections	20091	5501
Goodness-of-fit (GOF) on F^2	1.053	1.322
R indices (all data)	R_1 = 0.1255, wR_2 = 0.2484	R_1 = 0.1135, wR_2 = 0.2544

*4.3.6. Zinc di(6-benzhydryl-4-methyl-2-(5-chloro-benzoimidazol-2-yl)phenolate) (**C6**)*

The procedure was similar to that used for **C5**, but using **L6** (0.19 g, 0.45 mmol), affording **C6** in 78.4% (0.16 g, 0.18 mmol). IR (KBr; cm^{-1}): ν 3496, 3025, 1658, 1624, 1529, 1445, 1381, 1248, 1098, 1027, 754, 695. *Anal.* Calc. for $C_{54}H_{40}Cl_2N_4O_2Zn$: C, 71.02; H, 4.41; N, 6.14. Found: C, 71.14; H, 4.35; N, 6.09%.

4.4. X-ray crystallographic studies

Single crystals of complexes **C1** and **C4** suitable for an X-ray structural determination were grown by the slow diffusion of *n*-heptane into THF solution. X-ray studies were carried out on a Rigaku Saturn724+ CCD with graphite-monochromatic Mo Kα radiation (k = 0.71073 Å) at 173(2) K, cell parameters were obtained by global refinement of the positions of all collected reflections. Intensities were corrected for Lorentz and polarization effects and empirical absorption. The structures were solved by direct methods and refined by full-matrix least squares on F^2. All hydrogen atoms were placed in calculated positions. Structure solution and refinement were performed by using the SHELXL-97 package (Table 5) [42].

Acknowledgments

The authors thank the National Natural Science Foundation of China for support of this research (Grant No. 20773149). C.R. thanks the EPSRC for an Overseas Travel Grant.

Appendix A. Supplementary material

CCDC 863307 and 863308 contains the supplementary crystallographic data for this paper. These data can be obtained free of charge from The Cambridge Crystallographic Data Centre via www.ccdc.cam.ac.uk/data_request/cif. Supplementary data associated with this article can be found, in the online version, at http://dx.doi.org/10.1016/j.ica.2012.03.057.

References

[1] M.L. McKelvy, T.R. Britt, B.L. Davis, J.K. Gillie, F.B. Graves, L.A. Lentz, Anal. Chem. 70 (1998) 119R.
[2] S.K. Dogra, J. Mol. Struct. 734 (2005) 51.
[3] J.-G. Guo, Y.-M. Cui, H.-X. Lin, X.-Z. Xie, H.-F. Chen, J. Photochem. Photobio. A. 219 (2011) 42.
[4] M.N. Manjunatha, A.G. Dikundwar, K.R. Nagasundara, Polyhedron 30 (2011) 1299.
[5] S. Demirayak, I. Kayagil, L. Yurttas, Eur. J. Med. Chem. 46 (2011) 411.
[6] Z. Tian, W. Wu, W. Wan, A.D.Q. Li, J. Am. Chem. Soc. 133 (2011) 16092.
[7] G. Verdasco, M.A. Martín, B.de1. Castillo, P. López-Alvarado, J.C. Menéndez, Anal. Chim. Acta 303 (1995) 73.
[8] A.W. White, R. Almassy, A.H. Calvert, N.J. Curtin, R.J. Griffin, Z. Hostomsky, K. Maegley, D.R. Newell, S. Srinivasan, B.T. Golding, J. Med. Chem. 43 (2000) 4084.
[9] J.L. Morales, J. Krzeminski, S. Amin, G.H. Perdew, Chem. Res. Toxicol. 21 (2008) 472.
[10] L. Fabbrizzi, G. Francese, M. Licchelli, A. Perotti, A. Taglietti, Chem. Commun. (1997) 581.
[11] J. Kabatc, B. Jędrzejewska, A. Bajorek, J. Pączkowski, J. Fluoresc. 16 (2006) 525.
[12] R.N. Dsouza, U. Pischel, W.M. Nau, Chem. Rev. 111 (2011) 7941.
[13] S. Santra, G. Krishnamoorthy, S.K. Dogra, J. Mol. Struct. 559 (2001) 25.
[14] R. Yang, K. Li, K. Wang, F. Zhao, N. Li, F. Liu, Anal. Chem. 75 (2003) 612.
[15] Y. Zhang, R.H. Yang, F. Liu, K.A. Li, Anal. Chem. 76 (2004) 7336.
[16] M. Huang, P. Liu, Y. Chen, J. Wang, Z. Liu, J. Mol. Struct. 788 (2006) 211.
[17] H.J. Jung, N. Singh, D.O. Jang, Tetrahedron Lett. 49 (2008) 2960.
[18] Y.-P. Tong, S.-L. Zheng, X.-M. Chen, Eur. J. Inorg. Chem. (2005) 3734.
[19] G. Krishnamoorthy, S.K. Dogra, Spectrochim. Acta Part A Mol. Biomol. Spectrosc. 55 (1999) 2647.
[20] S.K. Dogra, J. Lumin. 118 (2006) 45.
[21] S. Banthia, A. Samanta, J. Phys. Chem. B. 110 (2006) 6437.
[22] P.C. Tway, L.J.C. Love, J. Phys. Chem. 86 (1982) 5223.
[23] T. Qiu, X. Xu, X. Qian, J. Photochem. Photobio. A. 214 (2010) 86.
[24] M.M. Oliva, J. Casado, J.T.L. Navarrete, J. Phys. Chem. C 111 (2007) 18778.
[25] M. Kurt, P.C. Babu, N. Sundaraganesan, M. Cinar, M. Karabacak, Spectrochim. Acta Part A Mol. Biomol. Spectrosc. 79 (2011) 1162.
[26] Ì. Sıdır, Y.G. Sıdır, Ì. Kayagil, Spectrochim. Acta Part A Mol. Biomol. Spectrosc. 81 (2011) 339.
[27] A.O. Eseola, W. Li, R. Gao, M. Zhang, X. Hao, T. Liang, N.O. Obi-Egbedi, W.-H. Sun, Inorg. Chem. 48 (2009) 9133.
[28] M. Forés, M. Duran, M. Solà, J. Phys. Chem. A 103 (1999) 4525.
[29] M. Mosquera, J.C. Penedo, M.C.R. Rodríguez, F. Rodríguez-Prieto, J. Phys. Chem. 100 (1996) 5398.
[30] M.M. Henary, C.J. Fahrni, J. Phys. Chem. A 106 (2002) 5210.
[31] Y.-P. Tong, S.-L. Zheng, X.-M. Chen, Inorg. Chem. 44 (2005) 4270.
[32] R.M. Tarkka, X. Zhang, S.A. Jenekhe, J. Am. Chem. Soc. 118 (1996) 9438.
[33] S. Park, J. Seo, S.H. Kim, S.Y. Park, Adv. Funct. Mater. 18 (2008) 726.
[34] S. Santra, G. Krishnamoorthy, S.K. Dogra, J. Mol. Struct. 559 (2011) 25.
[35] S. Santra, G. Krishnamoorthy, S.K. Dogra, Chem. Phys. Lett. 311 (1999) 55.
[36] S. Santra, S.K. Dogra, Chem. Phys. 226 (1998) 285.
[37] C.J. Fahrni, M.M. Henary, D.G. VanDerveer, J. Phys. Chem. A 106 (2002) 7655.
[38] W.R. Dawson, M.W. Windsor, J. Phys. Chem. 72 (1968) 3251.
[39] P. Hrdlovič, J. Kollár, S. Chmela, J. Photochem. Photobio. A. 163 (2004) 289.
[40] Ø.W. Akselsen, L. Skattebøl, T.V. Hansen, Tetrahedron Lett. 50 (2009) 6339.
[41] A.O. Eseola, W. Li, W.-H. Sun, M. Zhang, L. Xiao, J.A.O. Woods, Dyes Pigm. 88 (2011) 262.
[42] G.M. Sheldrick, SHELXTL-97, Program for the Refinement of Crystal Structures, University of Göttingen, Germany, 1997.